Lifetime Analysis of Metallized Polypropylene Capacitors in Modular Multilevel Converter Based on Finite Element Method

Yao, Ran; Li, Hui; Lai, Wei; Bahman, Amir Sajjad; Iannuzzo, Francesco

Published in:
IEEE Journal of Emerging and Selected Topics in Power Electronics

DOI (link to publication from Publisher):
10.1109/JESTPE.2020.2981806

Publication date:
2021

Document Version
Accepted author manuscript, peer reviewed version

Lifetime Analysis of Metallized Polypropylene Capacitors in Modular Multilevel Converter Based on Finite Element Method

Ran Yao, *Student Member IEEE*, Hui Li, Wei Lai, *Member IEEE*, Amir Sajjad Bahman, *Member IEEE*, and Francesco Iannuzzo, *Senior Member IEEE*

***Abstract*—Metallized polypropylene capacitors (MPPCs) are widely used in the modular multilevel converter (MMC) for high voltage direct current transmission systems, because of their lower power losses and self-healing capability. The performance of MPPCs in MMC deteriorates with time due to the increase of equivalent series resistance and decrease of capacitance. Therefore, the reliability analysis of MPPC is critical. This paper proposes a finite element method (FEM) to analyze the reliability of MPPC by considering corrosion failure. Firstly, the equivalent electric model and actual thermal model of the MPPC are established to calculate power losses and temperature distribution of the MPPC. Secondly, the corrosion failure of the MPPC is analyzed and simulated by the FEM model, the lifetime model of MPPC is established by the aging model of polypropylene film, and is verified by the traditional life-time model of corrosion failure and the floating aging tests. Finally, the voltage of each sub-module (SM) is extracted in the MMC model, and the lifetime of MPPCs in each SM is analyzed combining the FEM model and the lifetime model. The results show that in the MMC, the SMs in each arm near the DC line or the middle part have a lower lifetime of MPPCs.**

***Index Terms*—Corrosion failure, finite element method, lifetime prediction, metallized polypropylene power capacitors.**

I. Introduction

Metallized polypropylene capacitors (MPPCs) are commonly used in the modular multilevel converter (MMC) due to their advantages of high current carrying and self-healing capability [1,2]. However, some studies have shown that the failure rate of capacitors used in electrical power converter occupies about 30% [3]. Hence, the reliability analysis of MPPCs is critical for the safe and robust design of the converter. During the aging process, the equivalent series resistance (ESR) increases and the capacitance decreases in the MPPCs, which eventually leads to failure of MPPCs and threatens the safe operation of MMC [4]. The MPPCs are mainly composed of polypropylene films and electrodes, and the thicknesses of polypropylene films and electrodes are 6 μm -17 μm and 20 nm-40 nm, respectively, the volume of polypropylene film takes more than 90% in the MPPCs [5]. Thus, the aging of the polypropylene film is important to analyze the reliability of the MPPCs, and the voltage and the temperature are the main factors affecting the lifetime of polypropylene film [6]. In order to analyze the reliability of the MPPCs, it is necessary to find the degrading process of voltage and temperature in the MPPCs and the lifetime model of the polypropylene film.

In recent years, many researchers have studied the effects of MPPCs lifetime on temperature and voltage. In [7], some experimental results have shown that the lifetime of MPPCs decreases with increasing of temperature and voltage. M. Makdessi et al. do some aging experiments; the results have shown that voltage and temperature affect the capacitance of the MPPCs [8]. But all the results are based on the MPPCs aging experiments, which take thousands of hours. In order to save time, a simulation method is needed to analyze the heat flow and voltage/current distribution during the aging process of the MPPCs. Z.W. Li et al. have built a thermal field model with a finite element method (FEM) to verify the temperature rise of a single MPPC during the aging process [9]. J. Ostrowski et al. have built an electric 3D-simulation model to analyze the electric potential of a single MPPC with a real structure [10]. However, in the thermal field model, the power loss of MPPC was calculated by a mathematical model without considering the electric field effect. In the electric field model, the whole MPPC model with all structures is very difficult to build, the researchers only construct some part of the MPPC, which is unable to extract the power loss of the total device. Therefore, it is necessary to build an electric model combining with the operating conditions to extract the power loss of the MPPC and calculate the temperature of MPPC through the

This work was supported in part by the National Key Research and Development Program of China under Grant 2018YFB0905803, in part by the National Natural Science Foundation of China – State Grid Corporation Joint Fund for Smart Grid under Grant U1966213, and in part by the Graduate Research and Innovation Foundation of Chongqing, China under Grant CYB18008. (*Corresponding author*: *Hui Li*; *Ran Yao*.)

R. Yao is the State Key Laboratory of Power Transmission Equipment & System Security and New Technology, School of Electrical Engineering, Chongqing University, Chongqing 400044, China, and also with the Department of Energy Technology, Aalborg University, Aalborg 9220, Denmark. (e-mail: yaoran1234@163.com).

H. Li, and W. Lai, are with the State Key Laboratory of Power Transmission Equipment & System Security and New Technology, School of Electrical Engineering, Chongqing University, Chongqing 400044, China (e-mail: cqulh@163.com; laiweicqu@126.com).

F. Iannuzzo and A. S. Bahman are with the Department of Energy Technology, Aalborg University, Aalborg 9220, Denmark (e-mail: fia@et.aau.dk; amir@et.aau.dk).

thermal field model.

At present, the reliability evaluation of MPPCs is mainly based on power cycling experiments and mathematical-statistical methods [11-13]. In [11], a Weibull statistic method has been used to calculate the failure rate of MPPCs. In [12,13], two mathematical methods have been used to calculate the reliability of MPPCs by considering capacitance loss. Q. Sun et al. have proposed a reliability assessment model for MPPCs based on degradation testing, which considers the degradation of MPPC capacitance [14]. H. Wang et al. use an empirical model to calculate the lifetime of MPPCs, which considers the effect of temperature and voltage stress [15]. L. P. Tomas discusses the effect of system harmonics and unbalanced loads on the reliability of capacitors, the harmonics and unbalanced loads reduce the lifetime of capacitors [16]. Although these methods consider the effects of capacitance, temperature, harmonics, and voltage on MPPCs lifetime, the operation conditions in these methods are constant, the influence of the aging process on MPPCs performance is not considered, and the effects of capacitance reduction on temperature and voltage during MPPCs aging are ignored. Thus, it is necessary to establish an MPPCs lifetime model and analyze the effect of capacitance on MPPCs performance during an aging process.

This paper is organized as follows. Section II provides an equivalent electric field model to analyze the electric stress and to extract the power loss of a single MPPC, and a thermal field model considers equivalent material parameters to calculate the temperature distribution of the MPPC. In section III, the corrosion failure is analyzed and simulated by FEM method, a lifetime model of MPPC is proposed by considering polypropylene film failure and verified by traditional lifetime model of corrosion failure and the floating aging tests. Section IV presents an MMC model to extract the voltage change of each MPPCs in sub-models (SMs), which is used to calculate the lifetime of all MPPCs in MMC. Section V concludes the paper.

II. Finite Element Modeling and Analysis

A. Electric field simulation of MPPC

A two-section MPPC in the MPPCs device is shown in Fig. 1. The two-section MPPC consists of a mandrel, sprayed-end, metallized polypropylene films, and electrodes. Two metallized polypropylene films are wound onto an insulating mandrel to create the MPPC, and each side is sprayed with metal zinc particles. The electrodes on the metallized polypropylene films are composed of aluminum (Al), zinc or aluminum-zinc alloy, and the layout of electrodes on the two metallized polypropylene films is different. The thickness values of the electrode and polypropylene are in nanometer ranges and micrometer ranges, respectively [5].

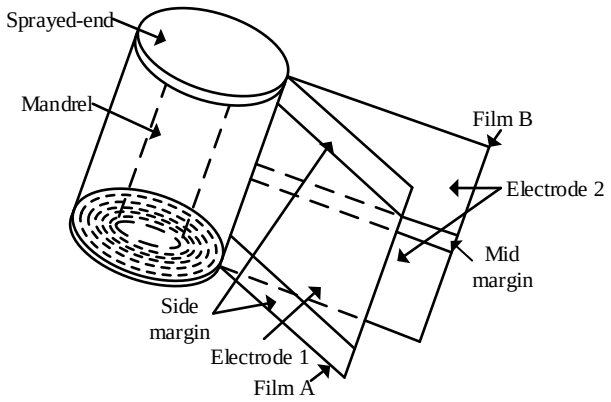

Fig. 1. Structure of a two-section MPPC.

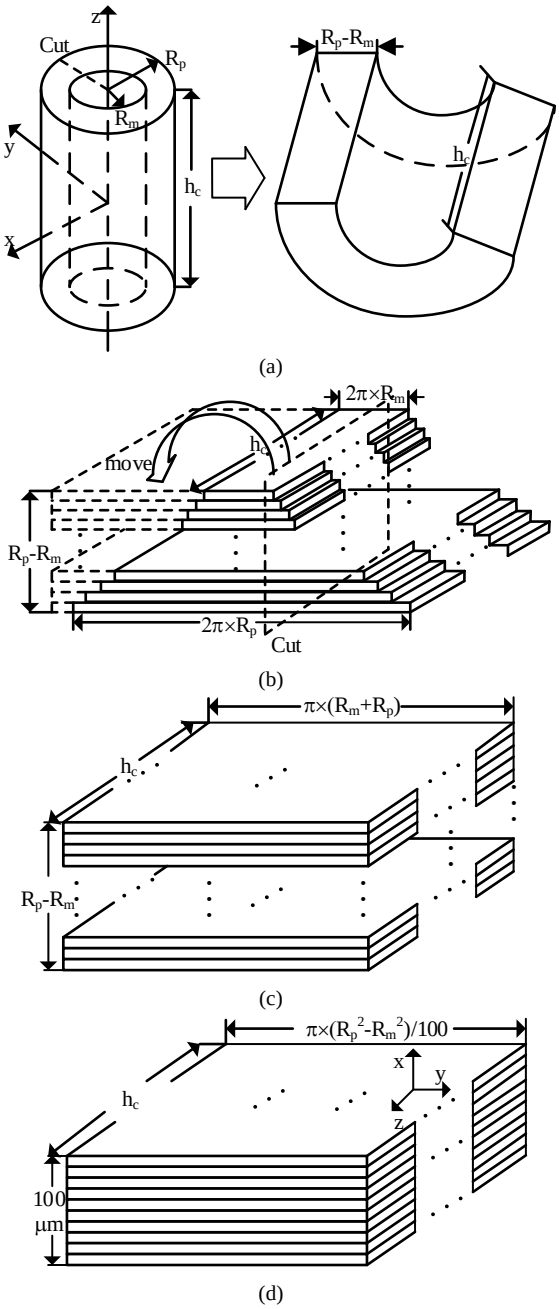

Fig. 2. Equivalent modeling of two-section MPPC. (a) the actual model; (b) the expand model with one radius cutting; (c) the equivalent model; (d) the simulation model.

The MPPC is made by stacking two metallized polypropylene films and winding them on the mandrel, each metallized polypropylene film has a thickness in the micrometer ranges and MPPC has a thickness in millimeter

ranges. Therefore, in the MPPC, more than 1000 layers of metallized polypropylene films stacked around the mandrel. If the two-section MPPC is constructed with the actual structure in the FEM model, the modeling method and the mesh elements are complicated and large, which is difficult for electrical filed simulation. Thus, an equivalent modeling method is proposed to simulate the electric field of the MPPC, as shown in Fig 2. In Fig. 2(a), the sprayed-ends and mandrel in the MPPC are ignored, the R_p is the radius of the MPPC, the R_m is the radius of the mandrel, h_c is the width of the metallized polypropylene film, z is the axial direction, x and y are the radial directions. Cut any radius in the MPPC, the expansion diagram is shown in Fig. 2(b). The metallized polypropylene films with different lengths are stacked together, the height of it is R_p-R_m, the width of it is h_c, the shortest length of it is $2\pi\times R_m$ and the longest length of it is $2\pi\times R_p$. Cut the lift area of the metallized polypropylene films and move it to the right side in Fig. 2(b). The new structures are shown in Fig 2(c), which consists of many metallized polypropylene films with the same length of $\pi\times(R_p+R_m)$, the height and the width in Fig. 2(c) have the same sizes in Fig 2(b). The simulation model of the MPPC is further simplified, as shown in Fig. 2(d), the height of the equivalent model changes to 100 μm, it is about 20 layers of the metallized polypropylene films. Keep the width and volume of the MPPC constant, the length of the MPPC equivalent model changes to $\pi\times(R_p^2-R_m^2)/100$ μm.

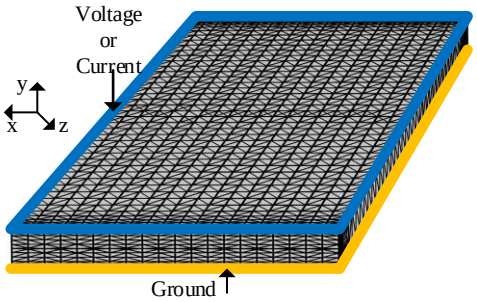

Fig. 3 The mesh result and the boundary condition of the MPPC.

The COMSOL 5.4 software is used for MPPC modeling. The mesh results and boundary conditions are shown in Fig. 3. The voltage/current is applied on one side of the MPPC and the other side connects to the ground. The x-axis size is enlarged by a factor of 10000 in Fig. 3, the physics-controlled mesh method with an element size of normal is used to mesh the equivalent model in the COMSOL. The number of body elements in the MPPC is 54488, and the number of boundary elements is 22896. In electric field simulation, a voltage or a current is applied to one sprayed-end, and another sprayed-end is connected to the ground.

TABLE I
MATERIALS PROPERTIES FOR ELECTRICAL SIMULATION

Material	Relative Permittivity (1)	Conductivity (S/m)
Polypropylene	2.2	5.5×10^{-13}
Aluminum	1 [29]	3.77×10^{7}

TABLE II
PARAMETERS FOR ELECTRICAL SIMULATION

Parameters	Unit	Value
Voltage	V	4400
Ground	V	0
Frequency	Hz	1000
Duty ratio	/	0.5

The electric filed simulation in COMSOL software considers three equations, which is the displacement current equation (1), the Ohm's law equation (2) and the electric field calculation equation (3), respectively.

$$\nabla\times\mathbf{J}=Q_j \tag{1}$$

$$\mathbf{J}=\sigma\times\mathbf{E}+jw\mathbf{D}+\mathbf{J}_e \tag{2}$$

$$\mathbf{E}=-\nabla\times V \tag{3}$$

Where ∇ is the operator of Laplace, $\mathbf{J}$ is the current density vector, Q_j is the distributed current source, σ is the conductivity, $\mathbf{E}$ is the electric field vector, $jw\mathbf{D}$ is the displacement current, $\mathbf{J}_e$ is the externally generated current density, V is the electric

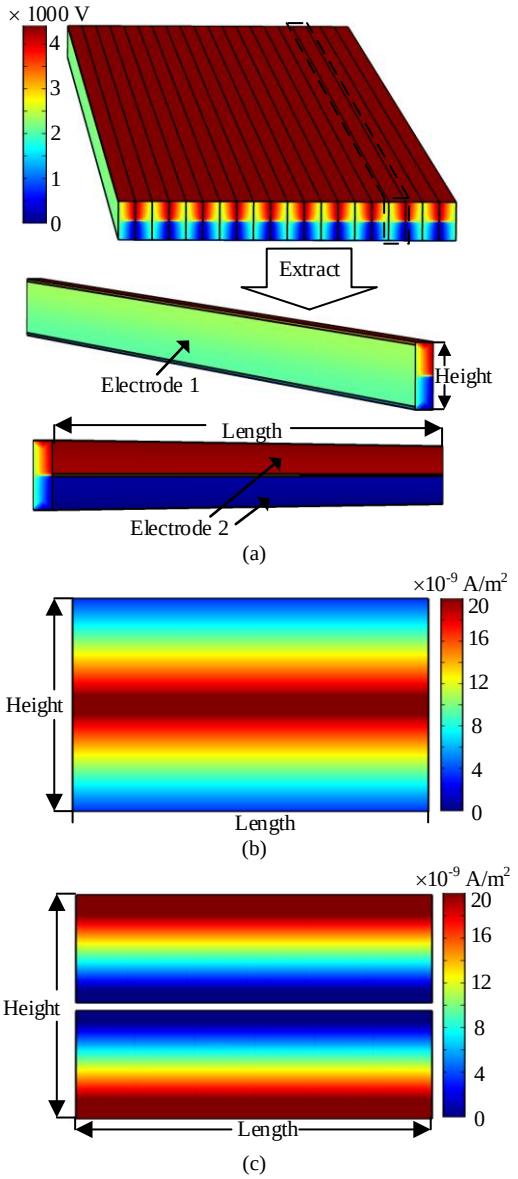

Fig. 4 Electric simulation results of the MPPC. (a) Voltage distribution in the MPPC model; (b) Current density in electrode 1; (c) Current density in electrode 2.

potential. Some material properties of the metallized polypropylene films for electrical simulation are listed in Table I [22, 29]. The electrical conductivity of the polypropylene is about 10^{-17} S/m to 10^{-12} S/m when the electric field strength higher than 10^{9} V/m, the electrical conductivity of the polypropylene is higher than 10^{-13} [28], the value of 5.5×10^{-13} S/m is used in the simulation. Some parameters setting in the simulation for electrical simulation are listed in Table II.

The electric simulation results of the MPPC are shown in Fig. 4. In Fig. 4(a), the voltage decreases from the one side (source) to the other side (ground). On the metallized polypropylene film both sides, the layout of electrode 1and electrode 2 is the same as that shown in Fig. 1, the electrode 1 has two side margins and the electrode 2 has a mid-margin. Between two metallized polypropylene films, the voltage decreases from the upper side of the electrode 2 toward the electrode 1. Then, the voltage decreases from the electrode 1 toward the lower side of the electrode 2. The height of the MPPC model is enlarged by a factor of 50 in Fig. 4(b) and Fig. 4(c). In Fig. 4(b), the current density of electrode 1 is lower on both sides and higher in the middle area. In Fig. 4(c), the current density of electrode 2 is lower in the middle area and higher on both sides. Therefore, the power loss on both sides of the metallized polypropylene film could be different. On the electrode 1, the voltage distribution is even and the current is higher in the middle area, the electrode 1 may generate more heat in the middle area. On the electrode 2, the voltage decreases from the upper side to the lower side, and the current is higher on the boundary side, the electrode 2 may generate more heat at the boundary side.

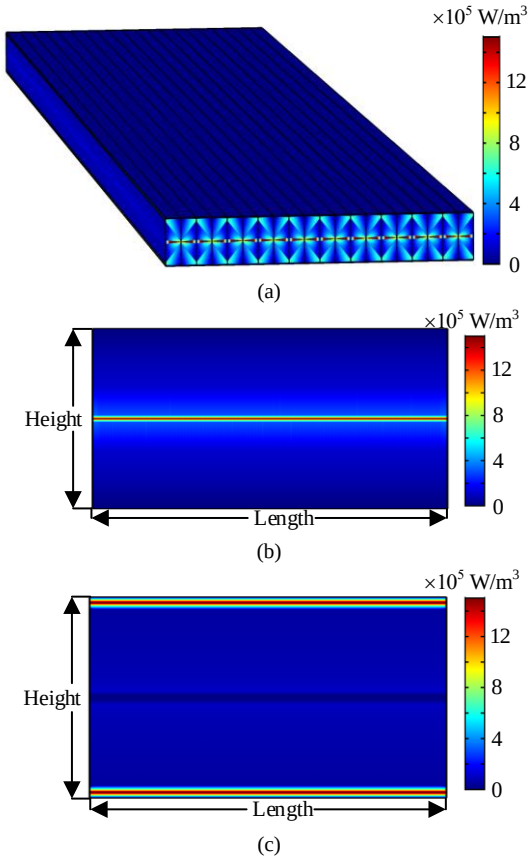

Fig. 5 Volume power density of the metallized polypropylene films. (a) Volume power density in the MPPC model; (b) Volume power density in electrode 1; (c) Volume power density in electrode 2.

B. *Thermal field simulation of MPPC*

To modify the thermal field distribution of two-section MPPC, the volume power density of the MPPC can be extracted by the electrical simulation results in the software, the volume power density of the MPPC is shown in Fig. 5. In Fig. 5(a), the volume power density is the highest in the middle part of the MPPC, the upper and lower sides have higher volume power density than other parts. In Fig. 5 (b), the volume power density in electrode 1 is the highest in the middle part and on both sides are the lowest. In Fig. 5(c), the volume power density in electrode 2 decreases from both sides to the middle part. The average volume power density of the model is about 51543 W/m^3.

Then, the actual MPPC model is used to the thermal simulation, the model and boundary conditions are shown in Fig. 6. In Fig. 6 (a), the actual MPPC model includes two sprayed-end, one mandrel, and metallized polypropylene film. The sprayed-end is made by zinc, the mandrel is made by Polycarbonate, the metallized polypropylene film consists of the Al electrodes and the polypropylene. The boundary conditions are shown in Fig. 6 (b), the heat source is applied in the metallized polypropylene film. The MPPC model operates with air cooling, the ambient temperature is fixed. The model meshes with the element size of fine, the number of body elements in the MPPC is 37938, and the number of boundary elements is 10776.

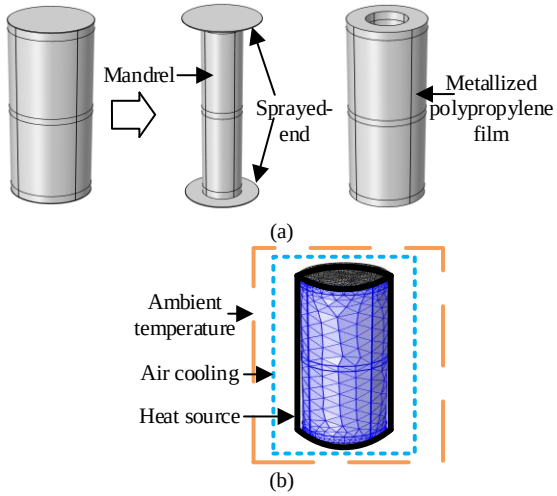

Fig. 6 Thermal simulation model and boundary conditions of the MPPC. (a) Actual MPPC simulation model; (b) Boundary conditions and mesh results.

In COMSOL software, the thermal field simulation considers the following three equations.

$$\rho\times C_p\times\frac{\partial T}{\partial t}+\rho\times C_p\times\mathbf{u}\times\nabla T+\nabla\times\mathbf{q}_{cond}=Q \tag{4}$$

$$\mathbf{q}_{cond}=-k\times\nabla\times T \tag{5}$$

$$-\mathbf{n}\times\mathbf{q}_{conv}=h\times(T_{ext}-T) \tag{6}$$

where ρ is the density, C_p is the specific heat capacity, T is the temperature, t is the time, $\mathbf{u}$ the velocity field defined by the translational motion sub-node when parts of the model are

moving in the material frame, the unit of it is m/s. $\mathbf{q}_{cond}$ is the heat flux of thermal conduction in the model, k is the thermal conductivity, $\mathbf{n}$ is the direction vector, $\mathbf{q}_{conv}$ is the heat flux of thermal convection on the boundary condition, h is the heat transfer coefficient, T_{ext} is the external temperature, Q is the total heat source. The MPPC model is fixed, $\mathbf{u}$=0 m/s. Equations (4) and (5) are used to calculate the thermal balance in the model by heat conduction. Equation (6) is used to calculate the thermal exchange in the boundary interface by heat convection.

Some material properties of the metallized polypropylene films for electrical simulation are listed in Table III [17, 29]. The metallized polypropylene film consists of the Al electrodes and the polypropylene, and the thicknesses of polypropylene and Al electrodes are 5 nm and 10 μm, respectively. The material properties of metallized polypropylene film can be calculated by an equivalent material calculation method in literature [17]. Some parameters setting in the simulation for electrical simulation are listed in Table IV.

TABLE III
MATERIALS PROPERTIES FOR THERMAL SIMULATION

Material	Density (kg/m^3)	Thermal conductivity (W/(m×K))	Specific heat capacity (J/(kg×K))
Polypropylene	900	0.22	1780
Aluminum	2700	238	900
Zinc (Sprayed-end)	7140	121	388
Polycarbonate (Mandrel)	1200	0.19	1170
metallized polypropylene film	905	0.24 (z direction) 0.36 (x, y direction)	905

TABLE IV
PARAMETERS FOR THERMAL SIMULATION

Parameters	Unit	Value
Ambient temperature	°C	15
Air cooling coefficient [5]	W/(m^2×K)	7
Heat source	W/m^3	51543

In Fig. 7(A), the steady-state simulation results show that the temperature decreases from the middle part to both sides, the temperature on both sides is about 6 °C lower than the temperature in the middle part. In Fig. 7 (b), in the MPPC, the highest temperature in the middle part of the metallized polypropylene film is about 37 °C. The temperature in the mandrel is about 34 °C, and it is 3 °C higher than the temperature in the sprayed-ends. Thus, the middle part of the metallized polypropylene film in the MPPC may be the weakest area and prone to failure.

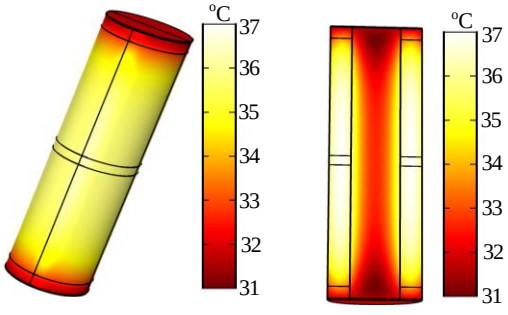

(a) (b)

Fig. 7 Thermal simulation results. (a) Temperature distribution of the MPPC; (b) Temperature distribution of the cross-section in the MPPC.

C. The simulation results verification

The accuracy of the equivalent electric model and the actual thermal model is verified by capacitance and temperature in the MPPC, respectively. The electric parameters of polypropylene are extracted in literature [18] and the geometric sizes of the MPPC get from the literature [9]. The capacitance of the MPPC can be calculated by equation (7) [19].

$$C=2\times\frac{\varepsilon_0\times\varepsilon_r\times l\times w}{d} \tag{7}$$

Where ε_0 is the vacuum permittivity, ε_r is the relative permittivity, l is the length of the metallized polypropylene film, w is the equivalent width of the two electrodes on the polypropylene film, d is the thickness of the metallized polypropylene film. The calculation result of the capacitance is 14.12 μF.

The capacitance in the equivalent electric model is shown in Fig.8. When the frequency is lower than 100 kHz, the capacitance of the MPPC remains stable, and then the capacitance of the MPPC drops sharply. When the frequency of the MPPC is lower than 100 kHz, the relative errors of capacitance between the equivalent model and the calculated value are below 1%. This can be used to verify the accuracy of the equivalent electric model.

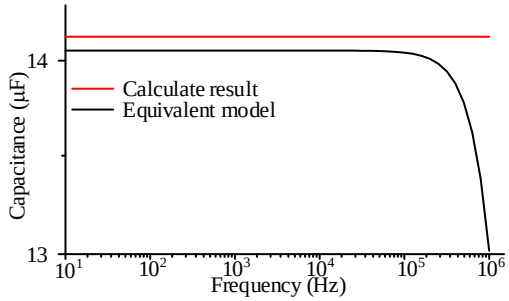

Fig. 8 The capacitance of the MPPC.

Under the same working conditions in literature [9], the currents of 298 A, 238 A and 170 A are simulated in the equivalent electrical model, and the volume power density in each current simulation result is extracted by the equivalent electric model. The maximum temperature distributions of different currents in the actual thermal model are shown in Fig 9. The temperature of the MPPC rises with the operation time. When the MPPC operates 70 mins, the temperature of the MPPC reaches the highest value. Compared with the experiment results in the literature [9], the simulation results have a high degree of fit with the experiment results, and the

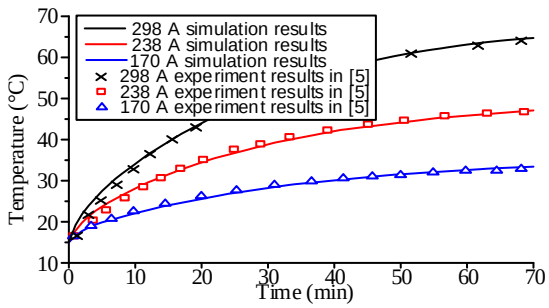

Fig. 9 Temperature simulation results of the MPPC.

relative temperature error is less than 2 °C. Thus, by extracting volume power density in the equivalent electric model, the actual thermal model can be used to simulate the temperature change of the MPPC during the operating time.

III. Corrosion Failure Simulation and Lifetime Modelling of MPPC

A. Corrosion failure of MPPCs

The corrosion failure is a main failure mode in the MPPCs when the MPPCs operate under high electric and thermal stress. If the external Al electrodes in the MPPCs has a lower pressure between two metallized polypropylene films, it is prone to corrosion damage, the Al will form to Al_2O_3. During the corrosion failure process, the corrosion parts progress from the heavy metal edge to the internal part on the metallized polypropylene film, the width of the electrode films is reduced [20, 21]. The heavy metal edge is the sprayed ends in this paper. The experiment results are shown in Fig. 10. In Fig 10 (a), the initial corrosion failure occurs from the heavy metal edge to the middle area. In Fig 10 (b), the corrosion failure forms the insulation corrosion gap between the heavy metal edge and metal film.

Due to the failure mechanism of the corrosion in the MPPC, the width of the electrodes on the metallized film is reduced, and the corrosion failure modeling method of the MPPC in the FEM model is shown in Fig. 11. In Fig. 11 (a), the width of the electrodes on the metallized films is unchanged before the corrosion failure of the MPPC. In Fig. 11 (b), the width of the electrodes on the metallized films is reduced by the corrosion failure, the Al in the corrosion failure area is changed to Al_2O_3, and the Al_2O_3 is not conductive. Thus, the corrosion failure parts become the insulator.

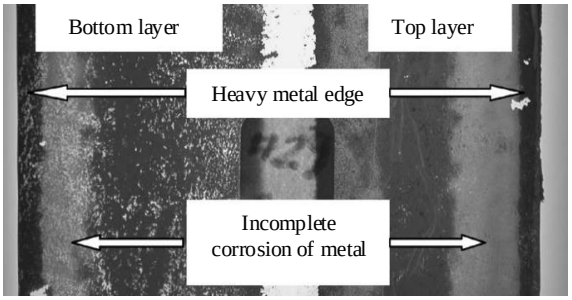

(a)

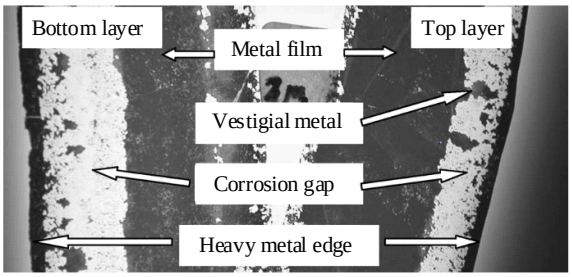

(b)

Fig. 10 The corrosion of metallized films in the MPPC. (a) Initial corrosion failure; (b) Corrosion failure.

The capacitance and ESR are related to the performance of the MPPC. In the corrosion failure process of the MPPC, the capacitance is decreasing and the ESR is increasing [22]. The capacitance of the MPPC can be extracted in the FEM model by COMSOL software. The ESR in MPPC can be calculated with equation (8) [23].

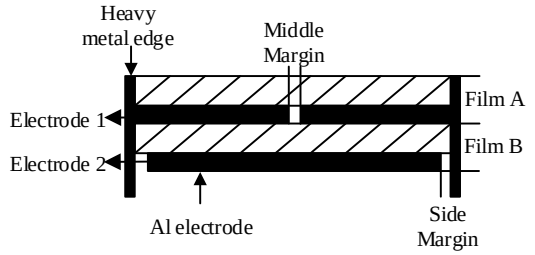

(a)

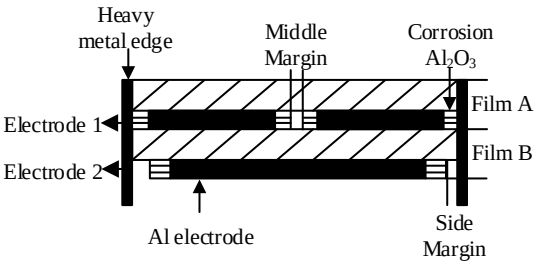

(b)

Fig. 11 The corrosion failure simulation in FEM. (a) The metallized films without corrosion failure; (b) The metallized films after corrosion failure.

$$ESR = R_{el} + \frac{DF}{2 \times \pi \times f \times C} \tag{8}$$

$$ESR = \frac{DF}{2 \times \pi \times f \times C} \tag{9}$$

Where the R_{el} is the resistance of the electrode, DF is the dissipation factor, the DF of polypropylene is about 5×10^{-4} at 1000 Hz [24], f is the operation frequency, and C is the capacitance of the MPPCs. The electrode resistance is very small in the MPPCs, thus, the ESR of the MPPCs can be changed to equation (9).

MPPC of C44PXGR5680RASK is selected as the case study for the lifetime modeling in the MMC system, the rated voltage is 2300V, the capacitance and ESR are 68 μF and 1.2 mΩ, respectively [25]. Simulation with 1 kHz, ambient temperature of 313 K and operation voltage of U/U_0=1, the capacitance, ESR and temperature change in the MPPC during the aging is shown in Fig. 12. Before corrosion failure, the capacitance and ESR of the MPPC extracted by the FEM model are 68.2 μF and 1.22 mΩ, respectively. In Fig. 12 (a), the capacitance decreases with the corrosion process in the MPPC. The corrosion length increases from 0 mm to 3mm, the capacitance of the MPPC decreases from 68.2 mF to 64.5 mF. The capacitance in the MPPC is reduced by 5.4 %. The ESR change trend in the MPPC is shown in Fig. 12 (b), the ESR increases with the corrosion process. The corrosion length increases from 0 mm to 3mm, the ESR of the MPPC increases from 1.22 mΩ to 1.25 mΩ. Thus, by simulating the change of corrosion length in the MPPC, different parameters can be extracted during corrosion failure in the FEM model of the MPPC. In Fig. 12 (c), the temperature of the MPPCs continue to grow during the aging process when the capacitance is

reduced by 5%, the temperature of the device rises from 40 °C to 110 °C.

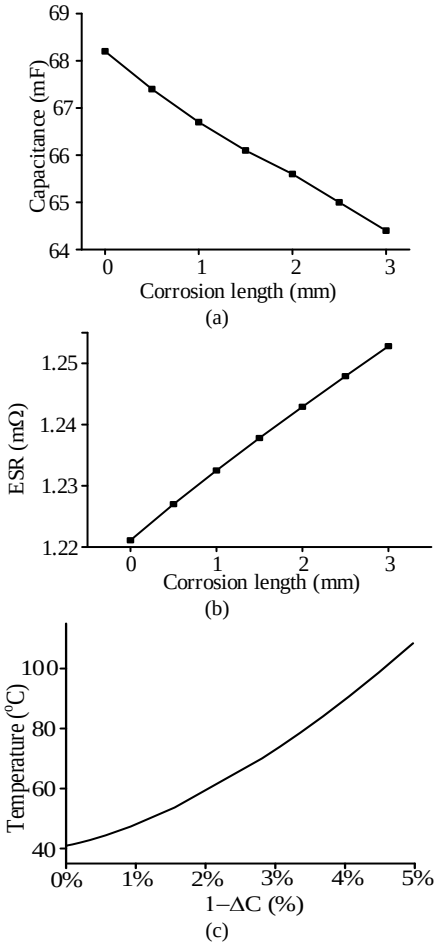

Fig. 12 The capacitance, ESR and temperature curve during corrosion failure. (a) The capacitance; (b) The ESR; (c) The temperature.

B. Corrosion failure of MPPC

During the corrosion failure, the capacitance of the MPPC decreases, and the failure criteria of the MPPC is the capacitance to reduce 5% [15]. The lifetime of the MPPC with the capacitance change can be calculated by equation (10) [22].

$$\Delta C(\%) = \frac{C_0 - k \times \sqrt{t}}{C_0} \times 100\% \tag{10}$$

where C_0 is the initial value of capacitance, k is a consistent parameter of corrosion failure, t is the operation time. Because the corrosion failure process is the oxidation process, and the kinetics of oxide layers approximately follows a parabolic law. By the theory of the oxidation kinetics of Wagner, the diffusion through the oxide film is limited by the process rate. Wagner's work showed that the development of an oxide layer at the interface between metal and gas follows a square root of time function [22]. Thus, some researches use square root time to build the lifetime model of the MPPC.

However, in this lifetime model, the effect of temperature and voltage on the lifetime of the MPPC cannot be reflected. Because the main element of the MPPCs is polypropylene films, the lifetime of MPPCs can be determined by the polypropylene film. By considering the voltage in the lifetime model of polypropylene film, the linear lifetime model of polypropylene film is calculated by equation (11) [26].

$$L_U = L_0 \times (\frac{U}{U_0})^{-\beta} \tag{11}$$

where U is the maximum voltage in operation condition, U_0 is the reference voltage, β is the coefficient, L_0 is the initial life of the MPPC. By considering the temperature in the lifetime model of polypropylene film, the lifetime model of the MPPC is calculated with the Arrhenius model as equation (12) [26].

$$L_T = L_0 \times \exp\left[-B \times (\frac{1}{K_R} - \frac{1}{K_T})\right] \tag{12}$$

where B is a fundamental parameter for thermal stress, and $B = A_k/k$, A_k is the activation energy of the aging process, k is the Boltzmann constant, K_R is the reference temperature, in this paper the value of K_0 is 313 K, K_T is the highest temperature in operation condition.

In the aging experiment, the lifetime of the MPPC is affected by temperature and voltage, when the temperature and voltage of the MPPC rise, the lifetime of the MPPC decreases [13-15]. Thus, the lifetime model of the MPPC should consider the effect of voltage and temperature. Combining equation (11) and equation (12), the lifetime of the MPPC can be calculated by equation (13).

$$L(U,T) = L_0 \times (\frac{U}{U_0})^{-\beta} \times \exp\left[-B \times (\frac{1}{K_R} - \frac{1}{K_T})\right] \tag{13}$$

To obtain the constant parameter of β and B in the lifetime model, the temperature acceleration factor and voltage acceleration factor are defined. The voltage acceleration factor is shown in equation (14), the value of K_T is equal to K_R, the U in the molecule is equal to U_0, the U in the denominator is a

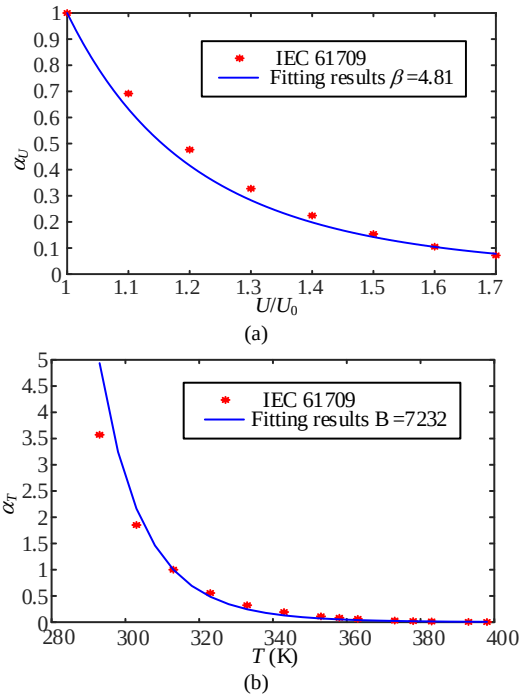

Fig. 13 Acceleration factor fitting results of the MPPC. (a) Voltage acceleration factor; (b) Temperature acceleration factor.

variable. The temperature acceleration factor is shown in equation (15), the value of U is equal to U_0, the K_T in the molecule is equal to K_R, the K_T in the denominator is a variable.

$$\alpha_U = \frac{L(U,K_0)}{L(U_0,K_0)} = \left(\frac{U}{U_0}\right)^{-\beta} \tag{14}$$

$$\alpha_T = \frac{L(U_0,K)}{L(U_0,K_0)} = \exp\left[-B\times\left(\frac{1}{K_0}-\frac{1}{K_T}\right)\right] \tag{15}$$

Extracting the temperature and voltage acceleration factor value of the MPPCs from IEC standard 61709 [27], the fitting line results by using MATLAB are shown in Fig. 13.

In Fig. 13 (a), when the K_T=313 K, the voltage acceleration factor decreases with the rise of operation voltage, and the value of β is 4.81. In Fig. 13 (b), when the U/U_0=1, the temperature acceleration factor decreases with the rise of operation temperature, the value of B is 7232. Considering the MPPCs used in the MMC system, the working voltage is around 2100 V. When the MPPCs operates with K_T= 333 K and U/U_0=1, the lifetime of the MPPC is about 140,000 h as shown in datasheet [25]. The initial lifetime L_0 of the MPPC is about 550,000 h, calculated with the operation conditions of K_T =313 K and U/U_0=1. Thus, the lifetime model of the MPPCs can be expressed by the following equation (16). The lifetime prediction of the MPPCs in different operating conditions is shown in Fig. 14. In Fig. 14, the lifetime of the MPPC decreases with temperature and voltage increase.

$$L(U,T) = 5.5\times10^5\times\left(\frac{U}{U_0}\right)^{-4.81}\times\exp\left[-7232\times\left(\frac{1}{K_0}-\frac{1}{K}\right)\right] \tag{16}$$

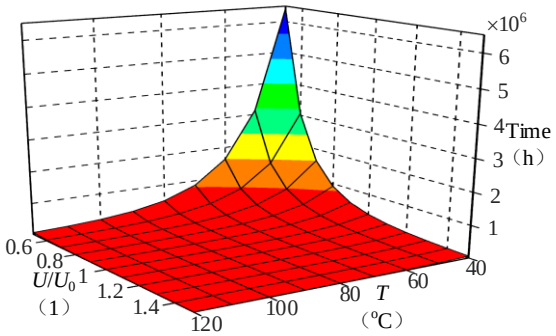

Fig. 14 The lifetime distribution of the MPPC.

To verify the lifetime model, the MPPC under different operation conditions is simulated by FEM model, the voltage and temperature are extracted to calculate the lifetime by equation (13), and the failure criteria of capacitance reduction 5 % in the MPPC is considered. By equation (10), the values of k with different operating conditions are shown in Fig. 15. The value of k increases with increasing of temperature and voltage, when the temperature is 380 K (around 100 °C) and U/U_0 is 1.1, the value of k is between 1.8×10^{-4} μF/s$^{0.5}$ and 2.7×10^{-4} μF/s$^{0.5}$. Compared with the experiment results in the literature [22], the operation conditions are 100 °C and U/U_0=1.1, the value of k is between 1×10^{-4} μF/s$^{0.5}$ and 6.9×10^{-4} μF/s$^{0.5}$. Thus, the value of k calculated by the lifetime model is within the range of value of k calculated by the experimental results, and the effectiveness of the lifetime model is verified.

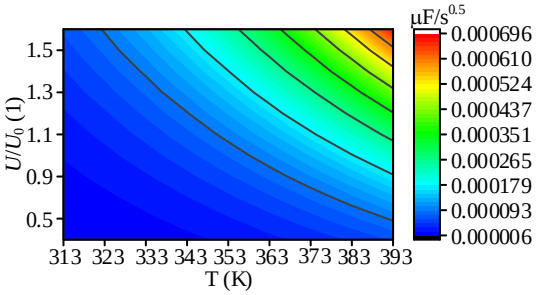

Fig. 15 the values of k with different operation conditions.

C. Experimental test

In order to identify the effectiveness of lifetime model, two same MPPC devices were performed with the floating aging tests, the experimental circuit is shown in Fig. 16. The rated voltage of the MPPC is 2200 V, the DC source applied 3960 V to the MPPC, U/U_0 is equal to 1.8. The MPPC is put in a thermostat, the ambient temperature is 90 °C. The capacitance of the MPPC is extracted every 24 hours.

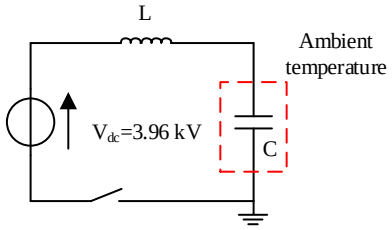

Fig. 16 Experiment circuit of floating aging test.

The experimental results are shown in Fig. 17. In test 1, the MPPC operates for about 48 hours, the capacitance drops by about 0.6 %. When the MPPC operates for more than 600 hours, the capacitance decreases by about 1%. After 900 hours of operation, the capacitance of the MPPC decreases rapidly, about 100 hours later, the capacitance decreases by about 5%. In test 2, the MPPC has been running for about 1000 hours with almost no change in capacitance, and then the capacitance of the MPPC decreases rapidly. After about 1100 hours, the capacitance reduced by 5 %. Compares the life of MPPC in the test and lifetime model. When the capacitance of the MPPC reduced by 5%, the lifetimes of MPPC in test 1 and test 2 are 1032 hours and 1128 hours, respectively. By simulating the same operating conditions in the proposed FEM model, the junction temperature of the MPPC is 94 °C, and the life of MPPC calculated by the lifetime model is 1086 hours. And the

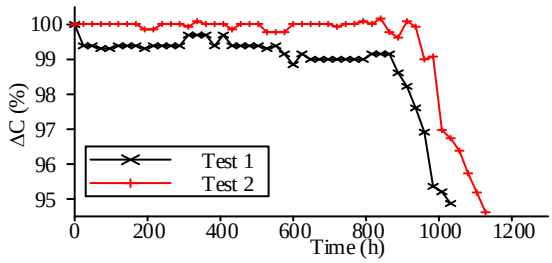

Fig. 17 Experiment results.

relative errors between the tests and lifetime model are 5 % and 3.9 %, respectively, the average error is about 4.5 %. Thus, the relative errors are very low, the effectiveness of the lifetime model is verified.

IV. Reliability Assessment of MPPCS in MMC

A. MMC model

Many researchers verified that the waveforms in the MMC-HVDC simulation model have a good fit with the experimental waveforms [30-32]. Thus, in order to analyze the reliability of MPPCs in the MMC system, the simulation model of MMC was established by using MATLAB/SIMULINK software. The topology of MMC is shown in Fig. 18, which includes three-phase units (arm A, arm B, and arm C), and each unit is divided into upper and lower arms (AU, BU, CU, AL, BL, CL). Each arm is composed of 20 identical SMs. The half-bridge topology is used in SM, it includes two IGBT modules (T1, T2), two FRD modules (D1, D2) and an MPPCs (C). Some operation parameters of the MMC system are listed in Table V.

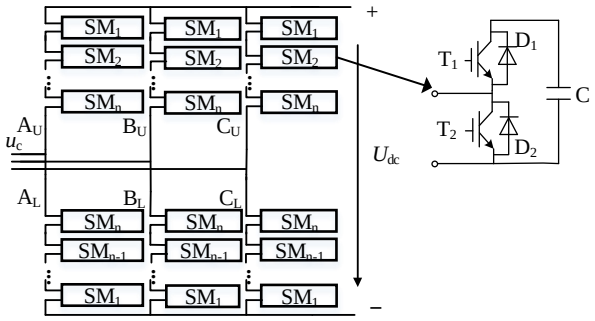

Fig. 18 The topology of MMC.

TABLE V
PARAMETERS OF THE MMC SYSTEM

Parameters	Value
MMC nominal power	50 MW
DC link voltage	41 kV
AC system nominal voltage	38 kV
Number of SM	20
Capacitance in each SM	2000 μF
Voltage of each MPPCs	2050 V
Normal frequency	50 Hz
Carrier frequency	800 Hz
Arm inductance	0.01 H
Arm resistance	0.004 Ω

The simulation results of the voltage waveform of the MPPCs in each SM in the AU between 0.54 s and 0.6 s are shown in Fig. 19. Although the voltage changing trend of each MPPCs is almost the same, the voltage value of each MPPCs still has some difference, the maximum value of each MPPCs has a difference of 40 V, and the minimum voltage of each MPPCs has a difference of 60 V. The average voltage value of each SM is shown in Table. VI.

The average voltage value of all MPPCs in A_U is 2050 V, and the average voltage value of each MPPCs is different. The average voltage value of SM 10 is the highest about 2072.27 V, and the average voltage value of SM 6 is the lowest about 2020.92 V. The different average voltage of each MPPCs produces different power loss, which leads to the different lifetime of MPPCs in each SM.

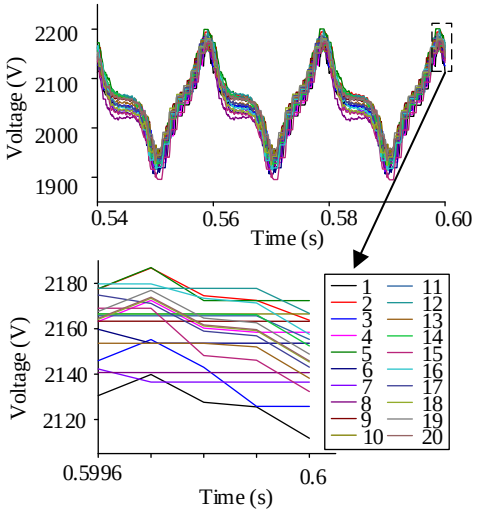

Fig. 19 Voltage waveforms of MPPCs in upper arms A.

TABLE VI
AVERAGE VOLTAGE VALUE OF EACH SM IN A_U

Number of SM	V_{ave} (V)	Number of SM	V_{ave} (V)
1	2052.59	11	2047.88
2	2062.14	12	2039.20
3	2061.78	13	2055.52
4	2030.48	14	2050.15
5	2055.20	15	2046.11
6	2020.92	16	2046.64
7	2038.40	17	2031.39
8	2067.70	18	2057.11
9	2043.35	19	2066.24
10	2072.27	20	2055.79

B. Reliability analysis of MPPCs in MMC

An MPPCs device with 72 single MPPC is used in the MMC, by extracting the MMC simulation results of average voltage and using the FEM method in section II, the temperature distribution of MPPCs in SM 1 upper arm A is shown in Fig. 20. The temperature on the outside of the MPPCs is about 40 °C, but the single MPPC in the middle part of the device has the highest temperature is 46 °C. The reliability of the MPPCs is affected by the weakest part. Thus, the highest temperature is used to calculate the lifetime of the MPPCs.

Combining with section II and section III, the reliability of the MPPCs in SM 1 is shown in Fig. 21. When the operation time is 0, the reliability of the MPPCs is 100 %. Before 10 years, the reliability of the MPPCs decreases slowly, which only

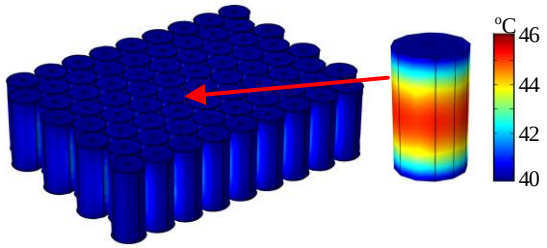

Fig. 20 Temperature distribution of MPPCs in SM 1upper arms A.

reduces about 40%. During 10 to 15 years, the reliability of the MPPCs drops rapidly, and the reliability of the MPPCs drops to 0 about 13.5 years.

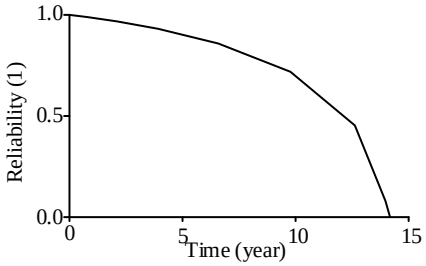

Fig. 21 The reliability of SM 1 in upper arms A.

Using the same method, the lifetime of all the MPPCs in MMC can be calculated as shown in Fig. 22. The average lifetime of the MPPCs in MMC is about 13.7 years. In Fig. 22 (a), comparing with the average voltage results in Table II, in upper arm A, the MPPC has lower average voltage, the lifetime of the MPPCs is higher. Divide all SMs in each arm into 5 parts as shown in Fig 22 (a) and Fig. 22 (b), the SMs in each Arm numbered 1 to 3 are part I, the SMs in each Arm numbered 4 to 7 are part II, the SMs in each Arm numbered 8 to 13 are part III, the SMs in each Arm numbered 14 to 17 are part IV, the SMs in each Arm numbered 18 to 20 are part V. The average lifetime of the MPPCs in each part is shown in Fig. 22 (c). The average lifetime of the MPPCs in part I and part III is below 13.7 years, and the average lifetime of the MPPCs in part II and part IV is above 13.7 years. The average lifetime of the MPPCs in part V is uneven. The number of SMs in part I is close to the DC line, and the number of SMs in part III is in the middle part of the MMC. Thus, the MPPCs near the DC line or the middle of the MMC system is weaker than that of other MPPCs.

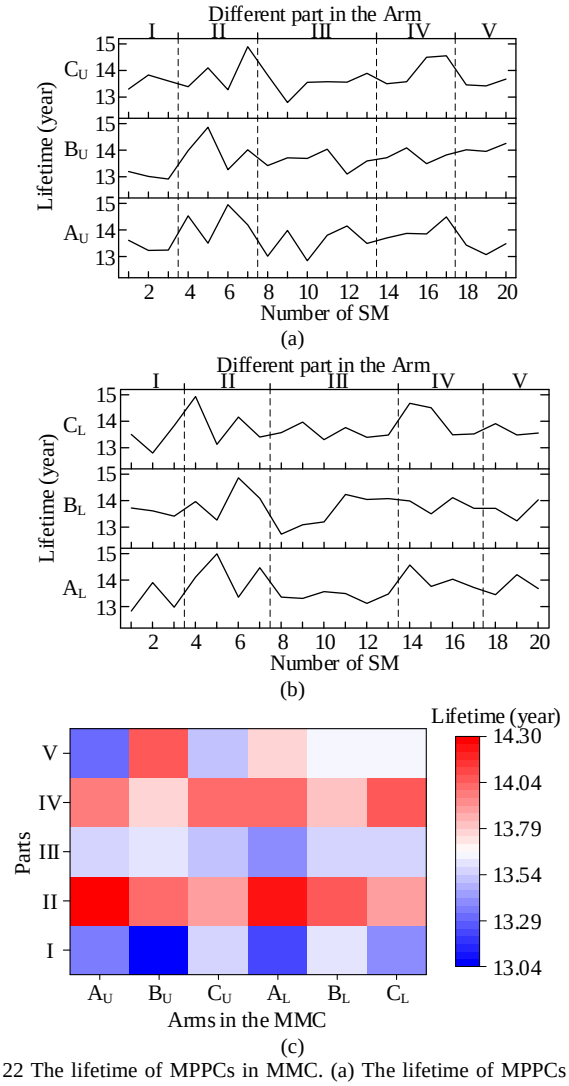

Fig. 22 The lifetime of MPPCs in MMC. (a) The lifetime of MPPCs in the upper arm; (b) The lifetime of MPPCs in the lower arm; (c) Average lifetime of different parts.

V. Conclusion

This paper proposed a FEM method to predict the lifetime of MPPCs in MMC by considering corrosion failure. The equivalent electric model is established to calculate the power loss of MPPC in actual operating conditions, and the thermal model is used to calculate the temperature of the MPPC. The electric and thermal models are verified by the capacitance equation and aging experiment results, respectively. Then, the corrosion failure of the MPPC is analyzed and simulated by the FEM method, the capacitance, ESR and temperature change during the corrosion failure are simulated. By considering the aging model of polypropylene film, the lifetime model of MPPC is built, the lifetime of the MPPC increases with decreasing of the voltage and temperature. The lifetime model is verified by the traditional lifetime model of corrosion failure and floating aging tests of the MPPC device, the experimental results are close to the calculated results, and the relative error is lower than 5%. Combining the FEM model and lifetime model, the lifetime distributions of all MPPCs in MMC are calculated, the SM has lower average voltage, the lifetime of MPPCs in this SM is higher. The SMs close to the DC line or in the middle of the MMC have a lower life of the MPPCs. This work could be useful for developing MPPSs lifetime prediction and health management for MMC systems, such as research on capacitor voltage equalization control, regular maintenance time of MPPC, and analyze the effects of capacitors aging on other power devices. The next steps are to build a more accurate model of the capacitor by considering the geometry and boundary conditions changes during the operation. Furthermore, more experiments will be performed at different conditions in order to better calibrate the lifetime model of the capacitor.

References

[1] Y. Tang, L. Ran, O. Alatise, and P. Mawby, “Capacitor Selection for Modular Multilevel Converter,” *IEEE Transactions on Industry Applications*, vol. 52, no. 4, pp. 3279–3293, 2016.

[2] Y. Tang, M. Chen, and L. Ran, “Design and control of a compact MMC submodule structure with reduced capacitor size using the stacked switched capacitor architecture,” Conference Proceedings - IEEE Applied Power Electronics Conference and Exposition - APEC, Long Beach, CA, USA, 2016.

[3] Y. Wu, and X. Du, “A VEN Condition Monitoring Method of DC-Link Capacitors for Power Converters,” IEEE Transactions on Industrial Electronics, vol. 66, no. 2, pp. 1296–1306, 2019.

[4] M. Makdessi, A. Sari, and P. Venet, “Health monitoring of DC link capacitors,” Chemical Engineering Transactions, vol. 33, pp. 1105–1110, 2013.

[5] M. Horak, and P. Mach, "Study of thermal ageing of polypropylene film capacitors". 2015 IEEE 21st International Symposium for Design and Technology in Electronic Packaging - SIITME, Brasov, Romania, 2015.
[6] B.X. Du, R.R. Xu, J. Li, H.L. Liu, M. Xiao, Z.L. Li, and Z.H. Hou, "Improved charging behaviors and flashover voltage of polypropylene film based on surface molecular structure modification," Thin Solid Films, vol. 680, pp. 12–19, 2019.
[7] Z. Li, H. Li, F. Lin, Y. Chen, D. Liu, B. Wang, and Q. Zhang, "Lifetime investigation and prediction of metallized polypropylene film capacitors," Microelectronics Reliability, vol. 53, no. 12, pp. 1962–1967, 2013.
[8] M. Makdessi, A. Sari, and P. Venet, "Metallized polymer film capacitors aging law based on capacitance degradation," Microelectronics Reliability, vol. 54, no. 9–10, pp. 1823–1827, 2014.
[9] Z.W. Li, H. Li, X. Huang, H.Y. Li, W.J. Wang, B.W. Wang, and Q. Zhang, "Temperature Rise of Metallized Film Capacitors in Repetitive Pulse Applications," IEEE Transactions on Plasma Science, vol. 43, no. 6, pp. 2038–2045, 2015.
[10] J. Ostrowski, R. Hiptmair, and H. Fuhrmann, "Electric 3D-simulation of metallized film capacitors,".4 COMPEL - The International Journal for Computation and Mathematics in Electrical and Electronic Engineering, vol. 26, no. 2, pp. 524–543, 2007.
[11] R. Gallay, "Metallized film capacitor lifetime evaluation and failure mode analysis,". CERN in the Proceedings of the CAS-CERN Accelerator School: Power Converters, Baden, Switzerland, 2014.
[12] Z.W Li, H. Li, F.C Lin, Y.H Chen, D. Liu, B.W Wang, Q. Zhang, and W. He, "Lifetime prediction of metallized film capacitors based on capacitance loss," IEEE Transactions on Plasma Science, vol. 41, no. 5, pp. 1313–1318, 2013.
[13] J.Y. Zhao, and F. Liu, "Reliability assessment of the metallized film capacitors from degradation data," Microelectronics Reliability, vol. 47, no. 2–3, pp. 434–436, 2007.
[14] Q. Sun, Y.Z. Tang, J. Feng, and T.D. Jin, "Reliability assessment of metallized film capacitors using reduced degradation test sample," Quality and Reliability Engineering International, vol. 29, no. 2, pp. 259–265, 2013.
[15] H. Wang, and F. Blaabjerg, "Reliability of capacitors for DC-link applications in power electronic converters- An overview," IEEE Transactions on Industry Applications, vol. 50, no. 5, pp. 3569–3578, 2014.
[16] T. Lledo-Ponsati, A.S. Bahman, F. Iannuzzo, D. Montesinos-Miracle, and S.G. Arellano, "Reliability Analysis of a 3-leg 4-wire Inverter under Unbalanced Loads and Harmonic Injection," 2019 20th Workshop on Control and Modeling for Power Electronics (COMPEL), Toronto, ON, Canada, 2019.
[17] Z.J. Wang, F. Yan, Z. Hua, L. Qi, Z. Hou, and Z. Xu, "Geometric optimization of self-healing power capacitor with consideration of multiple factors," Journal of Power Sources, vol. 323, pp. 147–157, 2016.
[18] M. Makdessi, A. Sari, G. Aubard, P. Venet, C. Joubert, and J. Duwattez, "Online health monitoring of metallized polymer film capacitors for avionics applications," IEEE International Symposium on Industrial Electronics, Buzios, Brazil, 2015.
[19] X. Qi, and S. Boggs, "Electrothermal failure of metallized film capacitor end connections-computation of temperature rise at connection spots," Journal of Applied Physics, vol. 94, no. 7, pp. 4449–4456, 2003.
[20] R.W Brown, "Linking corrosion and catastrophic failure in low-power metallized polypropylene capacitors," IEEE Transactions on Device and Materials Reliability, vol. 6, no. 2, pp. 326–333, 2006.
[21] R.W Brown, "Modeling of capacitor parameters related to the metal film layer with partial edge disconnection," IEEE Transactions on Components and Packaging Technologies, vol. 30, no. 4, pp. 774–780, 2007.
[22] M. Makdessi, A. Sari, P. Venet, P. Bevilacqua, and C. Joubert, "Accelerated ageing of metallized film capacitors under high ripple currents combined with a DC voltage," IEEE Transactions on Power Electronics, vol. 30, no. 5, pp. 2435–2444, 2015.
[23] G. Picci, and M. Rabuffi, "Status quo and future prospects for metallized polypropylene energy storage capacitors," PPPS 2001 - Pulsed Power Plasma Science 2001, Las Vegas, NV, USA,2001.
[24] P. Mach, M. Horák, and C. Stancu, "Thermal ageing of polypropylene film capacitors," 2015 38th International Spring Seminar on Electronics Technology, Eger, Hungary, 2015.
[25] Aluminum Can Power Film Capacitors, C44P-R, 2300 VDC, https://www.elfadistrelec.dk/en/power-film-capacitor-68uf-10-3kvdc-kemet-c44pxgr5680rask/p/30144936
[26] G.C. Montanari, and L. Simoni, "Aging Phenomenology and Modeling," IEEE Transactions on Electrical Insulation, vol. 28, no. 5, pp. 755–776, 1993.
[27] IEC Standard 61709-2017, pp46-47. https://webstore.iec.ch/publication/59985.
[28] V. Adamec, and J. H. Calderwood, "On the determination of electrical conductivity in polyethylene," Journal of Physics D: Applied Physics, vol. 14, no. 8, pp. 1487–1494, 1981.
[29] F. Capelli, J.R. Riba, and J. Sanllehí, "Finite element analysis to predict temperature rise tests in high-capacity substation connectors," IET Generation, Transmission and Distribution, vol. 11, no. 9, pp. 2283–2291, 2017.
[30] H. Makoto, and A. Hirofumi, "Control and Experiment of Pulsewidth-Modulated Modular Multilevel Converters," IEEE Transactions on Power Electronics, vol. 24, no. 7, pp. 1737–1747, 2009.
[31] Y. Tang, M. Chen, and L. Ran, "A Compact MMC Submodule Structure With Reduced Capacitor Size Using the Stacked Switched Capacitor Architecture," IEEE Transactions on Power Electronics, vol. 31, no. 10, pp. 6920-6937, 2016.
[32] E. Solas, G. Abad, J. A. Barrena, S. Aurtenetxea, A. Cárcar, and L. Zajac"Modular Multilevel Converter With Different Submodule Concepts—Part II: Experimental Validation and Comparison for HVDC Application," IEEE Transactions on Industrial Electronics, vol. 60, no. 10, pp. 4536-4546, 2013.